

# Impact of tensor force on quantum shell effects in quasifission reactions

Liang Li (李良)

*School of Nuclear Science and Technology, University of Chinese Academy of Sciences, Beijing 100049, China*

Lu Guo (郭璐)\*

*School of Nuclear Science and Technology, University of Chinese Academy of Sciences, Beijing 100049, China*

*Institute of Theoretical Physics, Chinese Academy of Sciences, Beijing 100190, China*

K. Godbey

*Facility for Rare Isotope Beams, Michigan State University, East Lansing, Michigan 48824, USA*

A. S. Umar

*Department of Physics and Astronomy, Vanderbilt University, Nashville, Tennessee 37235, USA*

---

## Abstract

Quantum shell effects drive many aspects of many-body quantal systems and their interactions. Among these are the quasifission reactions that impede the formation of a compound nucleus in superheavy element (SHE) searches. Fragment production in quasifission is influenced by shell effects as a nontrivial manifestation of microscopic dynamics hindering the full equilibration of the composite system to form the compound nucleus. In this Letter, we use the microscopic time-dependent Hartree-Fock (TDHF) theory to study  $^{48}\text{Ca}+^{249}\text{Bk}$  collisions to investigate the influence of the tensor component of the effective nucleon-nucleon interaction. The results show that the inclusion of the tensor force causes the spherical shell effect to become more prominent, particularly for the neutron number yield whose peak is exactly at magic number  $N = 126$ . This suggests that the tensor force plays a compelling role in the evolution of dynamical shell effects in nuclear reactions, influencing the competition between spherical and deformed shell gaps.

*Keywords:* TDHF, quasifission, tensor force

---

In the description of bound fermionic quantal systems, the presence of shells carries a particular importance as they determine the degree of stability of that system. This is especially relevant in nuclear physics, with protons and neutrons filling their respective shells with gaps between shells leading to the so-called magic numbers. These closed-shell nuclei are much more tightly bound compared to the ones that are non-magic and thus extremely stable [1, 2]. The largest neutron shell closures are believed to be at  $N = 126$  and possibly at  $N = 172$  or  $N = 184$ , and for protons near  $Z = 114$  and feasibly at higher values of  $Z = 120, 124$  or  $126$  [3, 4], with efforts to extend and confirm these with searches for the island of stability. In addition to the magic numbers of the spherical shells we also see deformation induced shell closures such as the ones at  $Z = 36$  [5] and  $Z = 40$ , and  $Z = 52-56$  observed in fission studies that are believed to be associated with octupole deformed shapes in the outgoing fission fragments [6, 7].

The synthesis of superheavy elements (SHE) has been a stimulating topic in the forefront of nuclear science [8]. To date, the

seventh row of the periodic table has been completed with the discovery of element  $Z = 118$ , Oganesson [9]. Despite this progress, it is still extremely difficult to produce SHE experimentally via cold or hot fusion reactions due to competing reactions that hinder the formation of the superheavy compound nucleus. Most significant of these are the fusion-fission and quasifission [10] reactions. Quasifission, as opposed to fusion, is a nonequilibrium process characterized by shorter interaction time, significant mass transfer, mass-angle correlations, and partial memory of the entrance channel [11, 12]. Theoretical studies of quasifission are an indispensable aid to elucidate the underlying reaction mechanisms due to the nontrivial interplay between the entrance and exit channels. Collision energy [13], deformation and orientation of the collision partners [14], neutron richness of the compound nucleus [15], and shell effects in the exit channel [16] all individually or collectively influence the quasifission dynamics. For example, an interesting phenomenon of quasifission reactions with actinide targets is that a mass-asymmetric yield peak in the  $^{208}\text{Pb}$  mass region was observed at beam energies around the Coulomb barrier [17–19]. In particular, the recent experiment simultaneously measured the atomic number and the mass of quasifission fragments and

---

\*Corresponding author

Email address: luguo@ucas.ac.cn (Lu Guo (郭璐))

demonstrated the important role of the proton shell closure at  $Z = 82$  in the quasifission fragment production [20].

A number of theoretical approaches have been developed that describe the quasifission in terms of multi-nucleon transfer processes [21–33]. Recently, time-dependent Hartree-Fock (TDHF) theory has proven to be an excellent tool for studying quasifission dynamics [34–36]. In particular, mass-angle distributions and final fragment total kinetic energies (TKE) [15, 16, 37–51] are in good agreement with experimental observations. Furthermore, TDHF studies of quasifission dynamics have taught us that dynamics itself may be dominated by shell effects [34, 52]. Despite the apparent strong differences between fission and quasifission, it is interesting to note that similar shell effects are found in both mechanisms [6, 7, 49, 53]. One benefit of utilizing microscopic calculations is that their only inputs are the parameters of the energy density functional. The parameters are usually fitted to nuclear structure properties only, consequently reaction calculations do not require additional parameters determined from the reaction mechanisms. In TDHF applications, the Skyrme interaction is employed as the effective nucleon-nucleon interaction [54] to construct the energy density functional. The full Skyrme interaction includes central, spin-orbit, and tensor terms, where the two-body tensor force is written as

$$\begin{aligned}
v_T = & \frac{t_e}{2} \left\{ [3(\sigma_1 \cdot \mathbf{k}')(\sigma_2 \cdot \mathbf{k}') - (\sigma_1 \cdot \sigma_2)\mathbf{k}'^2] \delta(\mathbf{r}_1 - \mathbf{r}_2) \right. \\
& + \delta(\mathbf{r}_1 - \mathbf{r}_2) [3(\sigma_1 \cdot \mathbf{k})(\sigma_2 \cdot \mathbf{k}) - (\sigma_1 \cdot \sigma_2)\mathbf{k}^2] \left. \right\} \\
& + t_o \left\{ 3(\sigma_1 \cdot \mathbf{k}') \delta(\mathbf{r}_1 - \mathbf{r}_2) (\sigma_2 \cdot \mathbf{k}) \right. \\
& \left. - (\sigma_1 \cdot \sigma_2) \mathbf{k}' \delta(\mathbf{r}_1 - \mathbf{r}_2) \mathbf{k} \right\}. \quad (1)
\end{aligned}$$

The coupling constants  $t_e$  and  $t_o$  represent the strengths of triplet-even and triplet-odd tensor interactions, respectively.

Historically, the full Skyrme interaction was often simplified due to computational cost. Early studies did not include the spin-orbit interaction, which led to the anomalies in fusion studies that was resolved by the inclusion of the spin-orbit terms [55, 56]. Until recently, most calculations in nuclear dynamics omitted the tensor part of the effective interaction. Only in the last few years, several studies showed the effect of tensor force on fusion barriers and cross sections [57–62]. The tensor force used in most dynamical calculations has been the SLy5t interaction [63], which includes the tensor component to the previously introduced SLy5 force [64]. In a recent investigation on Ni isotopes [65], by comparing the calculations with and without tensor force, it has been shown that the tensor part significantly affects the spin-orbit splitting of the proton  $1f$  orbit that may explain the survival of magicity far from the stability valley. The influence of the tensor force was also extensively studied in the superheavy region in Ref. [66].

In this Letter, the first evidence for the impact of the tensor force on shell effects is investigated for quasifission reactions using the TDHF theory.

The TDHF equations governing the time-evolution of the system are obtained variationally from a determinantal many-

body wavefunction,  $\Phi(t)$ , comprised of single-particle wave functions  $\phi_\lambda$

$$h(\{\phi_\mu\}) \phi_\lambda(r, t) = i\hbar \frac{\partial}{\partial t} \phi_\lambda(r, t) \quad (\lambda = 1, \dots, A), \quad (2)$$

where  $h$  is the resulting single-particle Hamiltonian deduced from the effective interaction. During the past decade it has become numerically feasible to perform TDHF calculations on a 3D Cartesian grid without any symmetry restrictions and with much more accurate numerical methods [67–69].

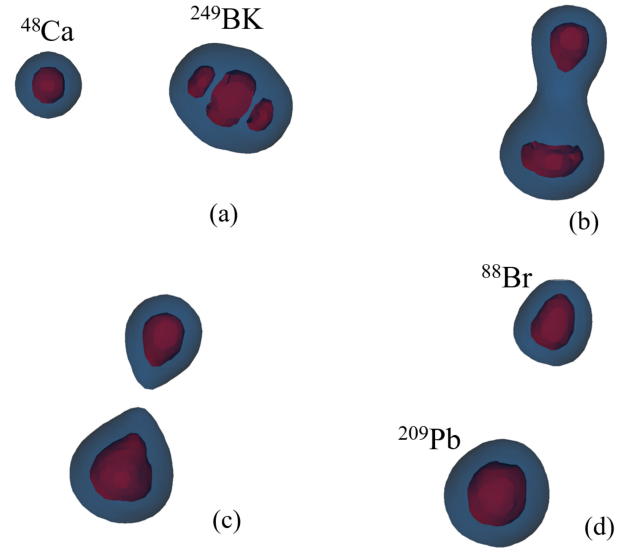


Figure 1: Isodensity surfaces at  $\rho = 0.03, 0.151 \text{ fm}^{-3}$  in midnight blue and red, respectively, for initial orientation  $\beta = 30^\circ$  and impact parameter  $b = 2 \text{ fm}$ , shown at times (a)  $t = 0$ , (b) 8.1, (c) 9.2, (d) 9.7 zs.

In this paper, we focus on quasifission in the reaction  $^{48}\text{Ca} + ^{249}\text{Bk}$ . The choice of this system was partially motivated by a recent extensive study of quasifission for the same system using the SLy4d interaction [49]. Static Hartree-Fock (HF) calculations result in a spherical density distribution for  $^{48}\text{Ca}$ , while  $^{249}\text{Bk}$  shows prolate quadrupole and hexadecupole deformation, in agreement with experimentally observed properties. In practice, TDHF calculations are performed by placing the two static HF solutions obtained for the target and projectile at a distance of 28 fm apart assuming that the two nuclei reached this separation on a Coulomb trajectory and the relevant velocities are used to boost the nuclei. The TDHF equations then propagate the nuclei in time as the reaction proceeds. In the case of quasifission the time evolution stops when the final fragments reach a separation of about 28 fm. The final scattering angle is then computed by extending the evolution to infinity on a Coulomb trajectory. For the dynamical evolution, we use a numerical box of  $60 \times 28 \times 48 \text{ fm}^3$ . The time step is set to be  $0.2 \text{ fm}/c$  and grid spacing is set to be  $1.0 \text{ fm}$ . For the placement of the prolate deformed  $^{249}\text{Bk}$  nucleus, after the ground state wave function is calculated we apply a rotation operator to the ground state using the b-spline interpolation method [70] to obtain wave functions of  $^{249}\text{Bk}$  for different orientations with respect to the collision axis. We have considered

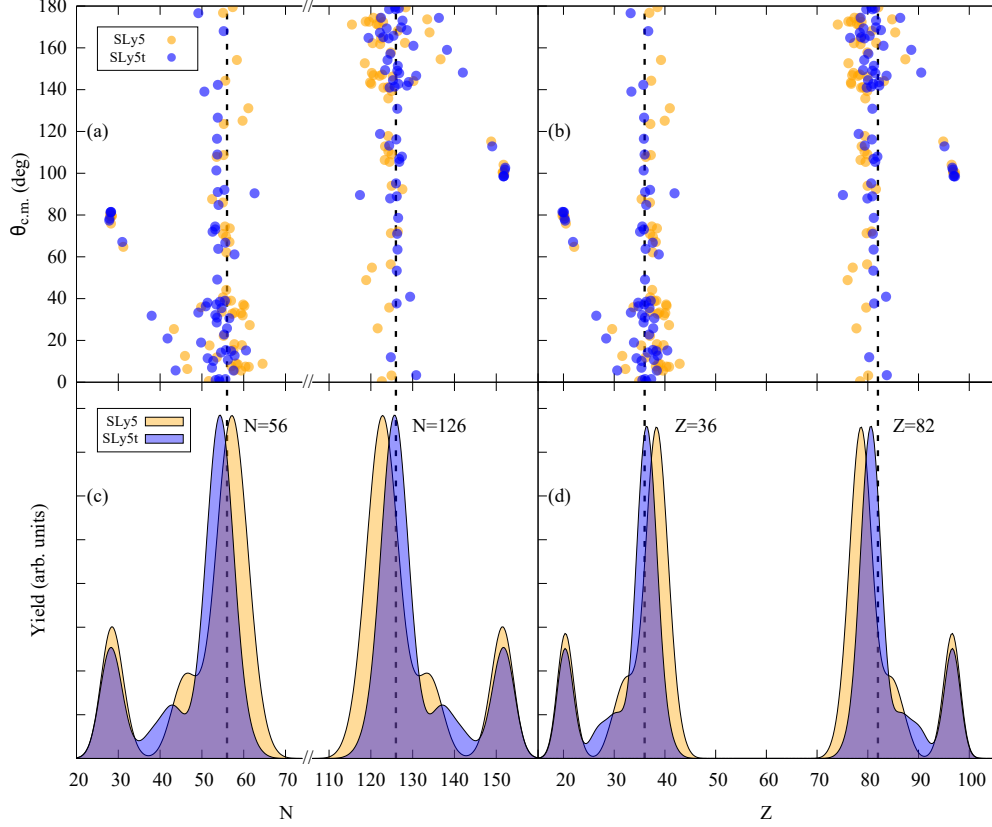


Figure 2: Quasifission reaction for  $^{48}\text{Ca}+^{249}\text{Bk}$  at  $E_{\text{c.m.}} = 234$  MeV. Distribution of scattering angle  $\theta_{\text{c.m.}}$  versus (a) neutron number  $N$ , (b) proton number  $Z$  with (blue points) and without (orange points) tensor force. Fragment (c) neutron number yield, (d) proton number yield with (blue shade) and without (orange shade) tensor force. The vertical dashed lines correspond to the spherical and deformed shell gaps at  $N = 56, 126$ , and  $Z = 36, 82$ , respectively.

the orientations of  $^{249}\text{Bk}$  for  $\beta = 0^\circ, 30^\circ, 45^\circ, 60^\circ, 90^\circ$  in the reaction plane. For each orientation calculations start at impact parameter  $b=0$  fm with a step  $\Delta b=0.5$  fm until the quasi-elastic reactions occur. One such collision is depicted in Fig. 1 corresponding to initial conditions  $b = 2$  fm and  $\beta = 30^\circ$ , shown at times (a)  $t = 0$ , (b) 8.1, (c) 9.2, (d) 9.7 zs. The light and heavy fragments are  $^{88}\text{Br}$  and  $^{209}\text{Pb}$ , respectively.

Depending on the contact time each quasifission run takes about 1.5-4 days on a 16 processors modern workstation using all processors in parallel. Results from different impact parameters and orientations have different contributions to the yield. We count the contributions using

$$\sigma_\lambda \propto \int_{b_{\min}}^{b_{\max}} b db \int_0^{\frac{\pi}{2}} d\beta \sin\beta P_b^{(\lambda)}(\beta), \quad (3)$$

where  $\lambda$  represents a specific reaction channel,  $P_b^{(\lambda)}(\beta)$  is the probability for a given impact parameter  $b$  and orientation  $\beta$ . Its value is 0 or 1 for the reaction channel  $\lambda$ .

Each point in Fig. 2(a) represents a TDHF result for reaction  $^{48}\text{Ca}+^{249}\text{Bk}$  at an impact parameter  $b$  and orientation  $\beta$ . The orange and blue points in Fig. 2(a)–(c) represent TDHF results using SLy5 and SLy5t Skyrme parameter sets. The only difference of the two sets is that SLy5t includes the tensor force term of the Skyrme effective interaction and SLy5 does not [63, 64]. The results of the two sets are then compared to address the

change that is caused by the tensor force. Figure 2(a) shows the correlations between scattering angle  $\theta_{\text{c.m.}}$  and neutron number  $N$ . We see more blue points lie on the vertical  $N = 126$  dashed line than orange points. Also, most orange points are on the left side of the  $N = 126$  line, except for the several rightmost points. This suggests that quasifission reactions with tensor force favor production of more fragments with neutron magic number  $N = 126$ . The neutron number of the rightmost points is  $N = 152$ , the same as the target  $^{249}\text{Bk}$ , corresponding to the trajectories where quasi-elastic reactions occur. With all the results from different orientations and impact parameters, it is possible to get smooth distributions of neutron and proton numbers in Fig. 2(c,d). In Fig. 2(c), the corresponding neutron number yield is plotted with (blue shade) and without (orange shade) tensor force. The peak of the blue shade is centered at  $N = 126$  while the peak of the orange shade is closer to  $N = 122$ . The yield distribution makes it more clear that the maximum production of heavy fragments with tensor force is affected by the  $N = 126$  shell closure. Fig. 2(b) shows the correlations between scattering angle  $\theta_{\text{c.m.}}$  and proton number  $Z$ . Blue points are systematically closer to the  $Z = 82$  line than orange points. This is also mirrored in the positions of yield peaks in Fig. 2(d). The peak of the blue shade is very close to  $Z = 82$  line while the peak of the orange shade is around  $Z = 79$ . This illustrates that  $Z = 82$  shell effects have greater

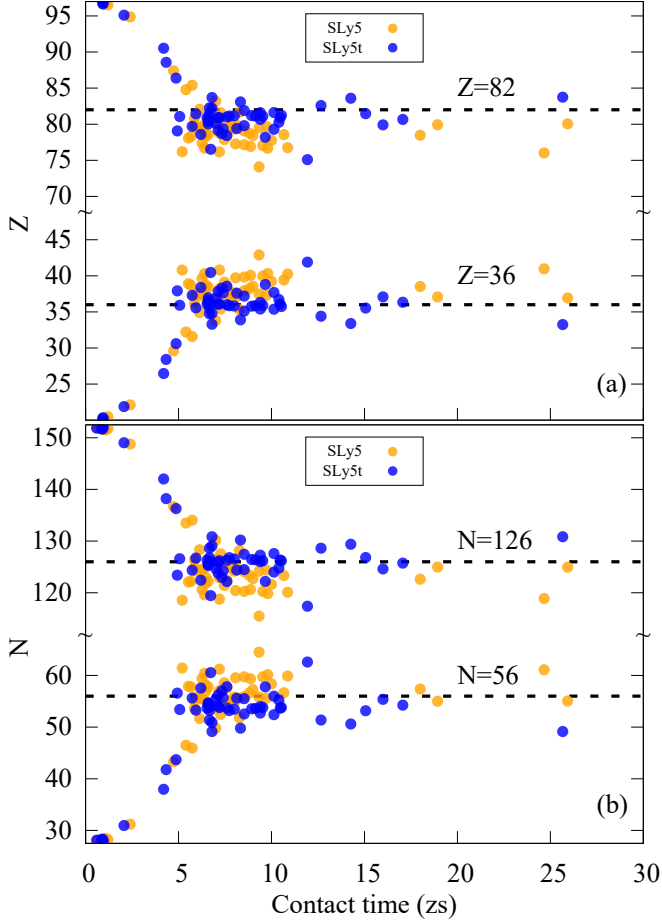


Figure 3: (a) Proton number  $Z$ , (b) neutron number  $N$  of quasifission fragments versus contact time with (blue points) and without (orange points) tensor force. The horizontal dashed lines represent spherical and deformed shell gaps.

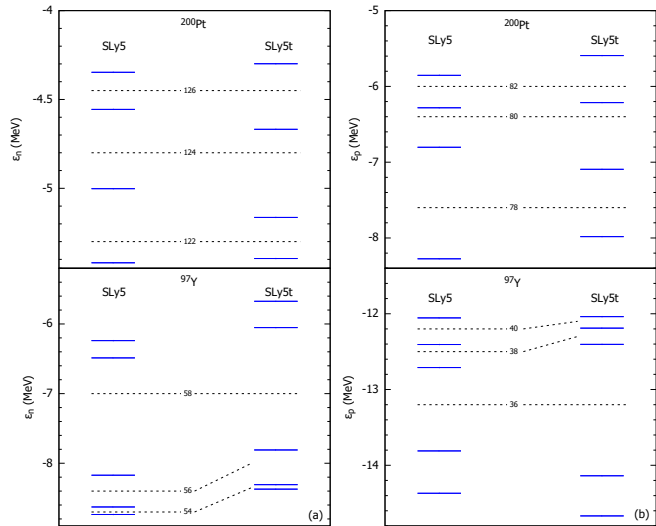


Figure 4: Single-particle energy levels for the heavy ( $^{200}\text{Pt}$ ) and light ( $^{97}\text{Y}$ ) fragments with SLy5 and SLy5t forces for neutrons (a) and for protons (b). Please see the full discussion in text for details.

impact on quasifission fragments with tensor force than those without tensor force.

Figure 3 shows the neutron and proton number of the heavy and light fragments as a function of the contact time. Contact time is defined as the time elapsed from the first touching of the target and projectile to the separation of the fragments (density overlap of about  $0.03 \text{ fm}^{-3}$ ). We observe that the charge of the heavy fragments with the tensor force (blue points) shifts towards the  $Z = 82$  shell gap compared to the calculations without the tensor force (orange points). This shift naturally impacts the charge of the light fragment, moving it from the deformed shell gap of  $Z = 40$  (zirconium) to  $Z = 36$  (krypton). As mentioned in the introduction this is a manifestation of the octupole deformed shapes [6] of the outgoing fragments. Similarly, the neutron number of heavy fragments shift upwards to the  $N = 126$  shell closure relative to the ones not using the tensor interaction. This pushes the neutron number of the light fragment towards  $N = 54$  from the no-tensor value of  $N = 56$ . Naturally, with a fixed number of neutrons and protons in the system the competing shell gaps influence each other for the formation of heavy and light fragments. From these we may conclude that spherical shell gaps compete with the deformed ones for fragment formation and this competition is sensitive to the details of the effective interaction employed. Finally, Fig. 3 also shows that the addition of the tensor force does not appreciably alter the contact time of the reactions, most occurring between 5-10 zs, which may be considered fast quasifission. Results using the SLy5 parameter set are consistent with Godbey *et al.*'s results using the SLy4d parameter set [49]. The SLy4d parameter set doesn't contain the tensor interaction, just as the SLy5 parameter set. Our results using the SLy5t parameter set show that, with the tensor force, the neutron shell effects play an important role and proton spherical shell effects become stronger. This has been observed experimentally with the spherical shell gap in quasifission for  $^{48}\text{Ti}+^{238}\text{U}$  [20] playing a vital role in fragment production.

The investigation of the shell effects at the single-particle level is complicated by the fact that the quasifission studies presented in the manuscript involve a distribution of points due to impact parameter and orientation angle variations. In some sense this resembles mass/charge distributions in an experimental study of QF or asymmetric fission, where the shell effects are deduced from the peaks of the distributions. In that sense this is different than a static structure study of gaps where for a given EDF one set of results exists or even from the traditional fission barrier calculations as a function of a deformation parameter for which one could clearly see the evolution of the gap from a single calculation. Dynamical evolution also has the problem that the single-particle energies contain the excitation energy of the system, which makes it hard to ascertain what the actual energy of the single-particle levels is. Despite of these difficulties we thought that one can investigate the deformation induced shell effects at the single particle level by removing the excitation energy from these levels. This was done by picking one of the points close to the SLy5 peak, taking the fragments after the scission point ( $^{97}\text{Y}$  and  $^{200}\text{Pt}$ ), and extracting the internal energies by keeping the shape of the fragments fixed using quadrupole and octupole deformation constraints of  $\beta_{20} = 0.552, 0.142$  and  $\beta_{30} = 0.049, 0.038$  for  $^{97}\text{Y}$  and  $^{200}\text{Pt}$ , re-

spectively. We have repeated the calculation for the same fragments using the SLy5t force. This is shown in Fig. 4 for neutrons and protons. We see that the effect of the tensor force is to enhance the  $N = 126$  gap for neutrons in the heavy fragment, while the neutron gaps for the light fragment remain about the same other than a shift. For protons we see a small enhancement of the  $Z = 82$  gap for the heavy fragment but a much larger enhancement of the  $Z = 36$  gap for the light fragment. While a limited study, these observations are consistent with our results.

The TDHF theory using the same Skyrme energy density functional with and without the tensor interaction was employed to simulate  $^{48}\text{Ca}+^{249}\text{Bk}$  collisions at a center-of-mass energy of 234 MeV. Calculations with five different orientations of the target have been combined to produce average fragment yield distributions. By comparing peaks of the yield distributions, we note that position of yield peaks moves towards magic number when the tensor force is included. Neutron-yield distributions in particular exhibit the most striking shift, with the yield peak moving to the neutron magic number  $N = 126$ . The differences caused by tensor force itself indicate that tensor force strengthens spherical shell effects, resulting in more quasifission fragments produced whose neutron numbers are around  $N = 126$  and whose proton numbers are closer to  $Z = 82$ . It is the first evidence that tensor force not only influences shell evolution in nuclear structure, but also plays a significant role in quasifission dynamics. This suggests further investigation on the role of tensor force in nuclear processes, as well as highlighting the delicate balance between spherical and deformed shell effects in nuclear dynamics.

This work has been supported by the Strategic Priority Research Program of Chinese Academy of Sciences (Grant No. XDB34010000 and No. XDPB15), the National Natural Science Foundation of China (Grants Nos. 11975237, 11575189, and 11790325), the U.S. Department of Energy under grant Nos. DE-SC0013847 (Vanderbilt University) and DE-SC0013365 (Michigan State University). The computations in present work have been performed on the HPC cluster in Beijing PARATERA Tech Ltd.

## References

- [1] W. D. Myers, W. J. Swiatecki, Nuclear masses and deformations, Nucl. Phys. 81 (1966) 1–60. doi:10.1016/0029-5582(66)90639-0.
- [2] A. Sobczewski, F. A. Gareev, B. N. Kalinkin, Closed shells for  $Z > 82$  and  $N > 126$  in a diffuse potential well, Phys. Lett. 22 (1966) 500–502. doi:10.1016/0031-9163(66)91243-1.
- [3] S. Ćwiok, J. Dobaczewski, P.-H. Heenen, P. Magierski, W. Nazarewicz, Shell structure of the superheavy elements, Nucl. Phys. A 611 (1996) 211–246. doi:10.1016/S0375-9474(96)00337-5.
- [4] A. T. Kruppa, M. Bender, W. Nazarewicz, P.-G. Reinhard, T. Vertse, S. Ćwiok, Shell corrections of superheavy nuclei in self-consistent calculations, Phys. Rev. C 61 (2000) 034313. doi:10.1103/PhysRevC.61.034313.
- [5] E. M. Kozulin, G. N. Knyazheva, I. M. Itkis, M. G. Itkis, Y. S. Mukhamejanov, A. A. Bogachev, K. V. Novikov, V. V. Kirakosyan, D. Kumar, T. Banerjee, M. Cheralu, M. Maiti, R. Prajapat, R. Kumar, G. Sarkar, W. H. Trzaska, A. N. Andreyev, I. M. Harca, A. Mitu, E. Vardaci, Fission of  $^{180,182,183}\text{Hg}^*$  and  $^{178}\text{Pt}^*$  nuclei at intermediate excitation energies, Phys. Rev. C 105 (2022) 014607. doi:10.1103/PhysRevC.105.014607.
- [6] G. Scamps, C. Simenel, Impact of pear-shaped fission fragments on mass-asymmetric fission in actinides, Nature 564 (2018) 382–385. doi:10.1038/s41586-018-0780-0.
- [7] G. Scamps, C. Simenel, Effect of shell structure on the fission of sub–lead nuclei, Phys. Rev. C 100 (2019) 041602(R). doi:10.1103/PhysRevC.100.041602.
- [8] Christoph E. Düllmann, Rolf–Dietmar Herzberg, Witold Nazarewicz, Yuri Oganessian, Special Issue on Superheavy Elements, Nucl. Phys. A 944 (2015) 1–690. doi:10.1016/j.nuclphysa.2015.11.004.
- [9] Yu. Ts. Oganessian, V. K. Utyonkov, Yu. V. Lobanov, F. Sh. Abdullin, A. N. Polyakov, R. N. Sagaidak, I. V. Shirokovsky, Yu. S. Tsyganov, A. A. Voinov, G. G. Gulbekian, S. L. Bogomolov, B. N. Gikal, A. N. Mezentsev, S. Iliiev, V. G. Subbotin, A. M. Sukhov, K. Subotic, V. I. Zagrebaev, G. K. Vostokin, M. G. Itkis, K. J. Moody, J. B. Patin, D. A. Shaughnessy, M. A. Stoyer, N. J. Stoyer, P. A. Wilk, J. M. Kenneally, J. H. Landrum, J. F. Wild, R. W. Lougheed, Synthesis of the isotopes of elements 118 and 116 in the  $^{249}\text{Cf}$  and  $^{245}\text{Cm} + ^{48}\text{Ca}$  fusion reactions, Phys. Rev. C 74 (2006) 044602. doi:10.1103/PhysRevC.74.044602.
- [10] E. Vardaci, M. G. Itkis, I. M. Itkis, G. Knyazheva, E. M. Kozulin, Fission and quasifission toward the superheavy mass region, J. Phys. G: Nucl. Part. Phys. 46 (2019) 103002. doi:10.1088/1361-6471/ab3118.
- [11] B. B. Back, R. R. Betts, K. Cassidy, B. G. Glagola, J. E. Gindler, L. E. Glendenin, B. D. Wilkins, Experimental Signatures of Quasifission Reactions, Phys. Rev. Lett. 50 (1983) 818–821. doi:10.1103/PhysRevLett.50.818.
- [12] W. Q. Shen, J. Albinski, A. Gobbi, S. Gralla, K. D. Hildenbrand, N. Herrmann, J. Kuzminski, W. F. J. Müller, H. Stelzer, J. Töke, B. B. Back, S. Bjørnholm, S. P. Sørensen, Fission and quasifission in U-induced reactions, Phys. Rev. C 36 (1987) 115–142. doi:10.1103/PhysRevC.36.115.
- [13] K. Nishio, S. Mitsuoka, I. Nishinaka, H. Makii, Y. Wakabayashi, H. Ikezoe, K. Hirose, T. Ohtsuki, Y. Aritomo, S. Hofmann, Fusion probabilities in the reactions  $^{40,48}\text{Ca} + ^{238}\text{U}$  at energies around the Coulomb barrier, Phys. Rev. C 86 (2012) 034608. doi:10.1103/PhysRevC.86.034608.
- [14] D. J. Hinde, M. Dasgupta, J. R. Leigh, J. P. Lestone, J. C. Mein, C. R. Morton, J. O. Newton, H. Timmers, Fusion-Fission versus Quasifission: Effect of Nuclear Orientation, Phys. Rev. Lett. 74 (1995) 1295–1298. doi:10.1103/PhysRevLett.74.1295.
- [15] K. Hammerton, Z. Kohley, D. J. Hinde, M. Dasgupta, A. Wakhle, E. Williams, V. E. Oberacker, A. S. Umar, I. P. Carter, K. J. Cook, J. Greene, D. Y. Jeung, D. H. Luong, S. D. McNeil, C. S. Palshetkar, D. C. Rafferty, C. Simenel, K. Stiefel, Reduced quasifission competition in fusion reactions forming neutron-rich heavy elements, Phys. Rev. C 91 (2015) 041602(R). doi:10.1103/PhysRevC.91.041602.
- [16] A. Wakhle, C. Simenel, D. J. Hinde, M. Dasgupta, M. Evers, D. H. Luong, R. du Rietz, E. Williams, Interplay between Quantum Shells and Orientation in Quasifission, Phys. Rev. Lett. 113 (2014) 182502. doi:10.1103/PhysRevLett.113.182502.
- [17] P. Gippner, K. D. Schilling, W. Seidel, F. Sary, E. Will, H. Sodan, S. M. Lukyanov, V. S. Salamatin, Y. E. Penionzhkevich, G. G. Chubarian, R. Schmidt, Shell effects in the evolution of the mass asymmetry in heavy-ion collisions leading to composite systems with  $Z=108$ , Z. Phys. A 325 (1986) 335–346. doi:10.1007/bf01294618.
- [18] M. G. Itkis, J. Äystö, S. Beghini, A. A. Bogachev, L. Corradi, O. Dorvaux, A. Gadea, G. Giardina, F. Hanappe, I. M. Itkis, M. Jandel, J. Kliman, S. V. Khlebnikov, G. N. Kniajeva, N. A. Kondratiev, E. M. Kozulin, L. Krupa, A. Latina, T. Materna, G. Montagnoli, Yu. Ts. Oganessian, I. V. Pokrovsky, E. V. Prokhorova, N. Rowley, V. A. Rubchenya, A. Ya. Rusanov, R. N. Sagaidak, F. Scarlassara, A. M. Stefanini, L. Stuttge, S. Szilner, M. Trotta, W. H. Trzaska, D. N. Vakhtin, A. M. Vinodkumar, V. M. Voskressenski, V. I. Zagrebaev, Shell effects in fission and quasi-fission of heavy and superheavy nuclei, Nucl. Phys. A 734 (2004) 136–147. doi:10.1016/j.nuclphysa.2004.01.022.
- [19] E. M. Kozulin, G. N. Knyazheva, I. M. Itkis, M. G. Itkis, A. A. Bogachev, L. Krupa, T. A. Loktev, S. V. Smirnov, V. I. Zagrebaev, J. Äystö, W. H. Trzaska, V. A. Rubchenya, E. Vardaci, A. M. Stefanini, M. Cinausero, L. Corradi, E. Fioretto, P. Mason, G. F. Prete, R. Silvestri, S. Beghini, G. Montagnoli, F. Scarlassara, F. Hanappe, S. V. Khlebnikov, J. Kliman, A. Brondi, A. Nitto, R. Moro, N. Gelli, S. Szilner, Investigation of the reaction  $^{64}\text{Ni} + ^{238}\text{U}$  being an option of synthesizing element 120, Phys. Lett. B 686 (2010) 227–232. doi:10.1016/j.physletb.2010.02.

- 041.
- [20] M. Morjean, D. J. Hinde, C. Simenel, D. Y. Jeung, M. Airiau, K. J. Cook, M. Dasgupta, A. Drouart, D. Jacquet, S. Kalkal, C. S. Palshetkar, E. Prasad, D. Rafferty, E. C. Simpson, L. Tassan-Got, K. Vo-Phuoc, E. Williams, Evidence for the Role of Proton Shell Closure in Quasifission Reactions from X-Ray Fluorescence of Mass-Identified Fragments, *Phys. Rev. Lett.* 119 (2017) 222502. doi:10.1103/PhysRevLett.119.222502.
- [21] G. G. Adamian, N. V. Antonenko, W. Scheid, Characteristics of quasifission products within the dinuclear system model, *Phys. Rev. C* 68 (2003) 034601. doi:10.1103/PhysRevC.68.034601.
- [22] Valery Zagrebaev, Walter Greiner, Shell effects in damped collisions: A new way to superheavies, *J. Phys. G: Nucl. Part. Phys.* 34 (2007) 2265. doi:10.1088/0954-3899/34/11/004.
- [23] Z.-Q. Feng, G.-M. Jin, J.-Q. Li, Production of heavy isotopes in transfer reactions by collisions of  $^{238}\text{U} + ^{238}\text{U}$ , *Phys. Rev. C* 80 (2009) 067601. doi:10.1103/PhysRevC.80.067601.
- [24] G.-F. Dai, L. Guo, E.-G. Zhao, S.-G. Zhou, Dissipation dynamics and spin-orbit force in time-dependent Hartree-Fock theory, *Phys. Rev. C* 90 (2014) 044609. doi:10.1103/PhysRevC.90.044609.
- [25] K. Zhao, Z. Li, Y. Zhang, N. Wang, Q. Li, C. Shen, Y. Wang, X. Wu, Production of unknown neutron-rich isotopes in  $^{238}\text{U} + ^{238}\text{U}$  collisions at near-barrier energy, *Phys. Rev. C* 94 (2016) 024601. doi:10.1103/PhysRevC.94.024601.
- [26] Z.-Q. Feng, Production of neutron-rich isotopes around  $N = 126$  in multinucleon transfer reactions, *Phys. Rev. C* 95 (2017) 024615. doi:10.1103/PhysRevC.95.024615.
- [27] F.-S. Zhang, C. Li, L. Zhu, P. Wen, Production cross sections for exotic nuclei with multinucleon transfer reactions, *Frontiers of Physics* 13 (2018) 132113. doi:10.1007/s11467-018-0843-6.
- [28] Z. Wu, L. Guo, Microscopic studies of production cross sections in multinucleon transfer reaction  $^{58}\text{Ni} + ^{124}\text{Sn}$ , *Phys. Rev. C* 100 (2019) 014612. doi:10.1103/PhysRevC.100.014612.
- [29] Z. Wu, L. Guo, Production of proton-rich actinide nuclei in the multinucleon transfer reaction  $^{58}\text{Ni} + ^{232}\text{Th}$ , *Sci. China-Phys. Mech. Astron.* 63 (2020) 242021. doi:10.1007/s11433-019-1484-0.
- [30] X. Jiang, N. Wang, Probing the production mechanism of neutron-rich nuclei in multinucleon transfer reactions, *Phys. Rev. C* 101 (2020) 014604. doi:10.1103/PhysRevC.101.014604.
- [31] L. Zhu, Shell inhibition on production of  $N = 126$  isotones in multinucleon transfer reactions, *Phys. Lett. B* 816 (2021) 136226. doi:10.1016/j.physletb.2021.136226.
- [32] Z. Wu, L. Guo, Z. Liu, G. Peng, Production of proton-rich nuclei in the vicinity of  $^{100}\text{Sn}$  via multinucleon transfer reactions, *Phys. Lett. B* 825 (2022) 136886. doi:10.1016/j.physletb.2022.136886.
- [33] X.-X. Sun, L. Guo, Microscopic study of compound-nucleus formation in cold-fusion reactions, *Phys. Rev. C* 105 (2022) 054610. doi:10.1103/PhysRevC.105.054610.
- [34] C. Simenel, A. S. Umar, Heavy-ion collisions and fission dynamics with the time-dependent Hartree-Fock theory and its extensions, *Prog. Part. Nucl. Phys.* 103 (2018) 19–66. doi:10.1016/j.pnpnp.2018.07.002.
- [35] P. D. Stevenson, M. C. Barton, Low-energy heavy-ion reactions and the Skyrme effective interaction, *Prog. Part. Nucl. Phys.* 104 (2019) 142–164. doi:10.1016/j.pnpnp.2018.09.002.
- [36] K. Godbey, A. S. Umar, Quasifission Dynamics in Microscopic Theories, *Front. Phys.* 8 (2020) 40. doi:10.3389/fphy.2020.00040.
- [37] David J. Kedziora, Cédric Simenel, New inverse quasifission mechanism to produce neutron-rich transfermium nuclei, *Phys. Rev. C* 81 (2010) 044613. doi:10.1103/PhysRevC.81.044613.
- [38] V. E. Oberacker, A. S. Umar, C. Simenel, Dissipative dynamics in quasifission, *Phys. Rev. C* 90 (2014) 054605. doi:10.1103/PhysRevC.90.054605.
- [39] P. M. Goddard, P. D. Stevenson, A. Rios, Fission dynamics within time-dependent Hartree-Fock: deformation-induced fission, *Phys. Rev. C* 92 (2015) 054610. doi:10.1103/PhysRevC.92.054610.
- [40] A. S. Umar, V. E. Oberacker, C. Simenel, Shape evolution and collective dynamics of quasifission in the time-dependent Hartree-Fock approach, *Phys. Rev. C* 92 (2015) 024621. doi:10.1103/PhysRevC.92.024621.
- [41] A. S. Umar, V. E. Oberacker, Time-dependent HF approach to SHE dynamics, *Nucl. Phys. A* 944 (2015) 238–256. doi:10.1016/j.nuclphysa.2015.02.011.
- [42] A. S. Umar, V. E. Oberacker, C. Simenel, Fusion and quasifission dynamics in the reactions  $^{48}\text{Ca} + ^{249}\text{Bk}$  and  $^{50}\text{Ti} + ^{249}\text{Bk}$  using a time-dependent Hartree-Fock approach, *Phys. Rev. C* 94 (2016) 024605. doi:10.1103/PhysRevC.94.024605.
- [43] E. Prasad, A. Wakhle, D. J. Hinde, E. Williams, M. Dasgupta, M. Evers, D. H. Luong, G. Mohanto, C. Simenel, K. Vo-Phuoc, Exploring quasifission characteristics for  $^{34}\text{S} + ^{232}\text{Th}$  forming  $^{266}\text{Sg}$ , *Phys. Rev. C* 93 (2016) 024607. doi:10.1103/PhysRevC.93.024607.
- [44] N. Wang, L. Guo, New neutron-rich isotope production in  $^{154}\text{Sm} + ^{160}\text{Gd}$ , *Phys. Lett. B* 760 (2016) 236–241. doi:10.1016/j.physletb.2016.06.073.
- [45] K. Sekizawa, K. Yabana, Time-dependent Hartree-Fock calculations for multinucleon transfer and quasifission processes in the  $^{64}\text{Ni} + ^{238}\text{U}$  reaction, *Phys. Rev. C* 93 (2016) 054616. doi:10.1103/PhysRevC.93.054616.
- [46] Chong Yu, Lu Guo, Angular momentum dependence of quasifission dynamics in the reaction  $^{48}\text{Ca} + ^{244}\text{Pu}$ , *Sci. China Phys.* 60 (2017) 092011. doi:10.1007/s11433-017-9063-3.
- [47] L. Guo, C. Shen, C. Yu, Z. Wu, Isotopic trends of quasifission and fusion-fission in the reactions  $^{48}\text{Ca} + ^{239,244}\text{Pu}$ , *Phys. Rev. C* 98 (2018) 064609. doi:10.1103/PhysRevC.98.064609.
- [48] X. Li, Z. Wu, L. Guo, Entrance-channel dynamics in the reaction  $^{40}\text{Ca} + ^{208}\text{Pb}$ , *Sci. China-Phys. Mech. Astron.* 62 (2019) 122011. doi:10.1007/s11433-019-9435-x.
- [49] K. Godbey, A. S. Umar, C. Simenel, Deformed shell effects in  $^{48}\text{Ca} + ^{249}\text{Bk}$  quasifission fragments, *Phys. Rev. C* 100 (2019) 024610. doi:10.1103/PhysRevC.100.024610.
- [50] K. Sekizawa, Microscopic description of production cross sections including deexcitation effects, *Phys. Rev. C* 96 (2017) 014615. doi:10.1103/PhysRevC.96.014615.
- [51] K. Sekizawa, K. Hagino, Time-dependent Hartree-Fock plus Langevin approach for hot fusion reactions to synthesize the  $Z = 120$  superheavy element, *Phys. Rev. C* 99 (2019) 051602. doi:10.1103/PhysRevC.99.051602.
- [52] Kazuyuki Sekizawa, TDHF Theory and Its Extensions for the Multinucleon Transfer Reaction: A Mini Review, *Front. Phys.* 7 (2019) 20. doi:10.3389/fphy.2019.00020.
- [53] C. Simenel, P. McGlynn, A. S. Umar, K. Godbey, Comparison of fission and quasi-fission modes, *Phys. Lett. B* 822 (2021) 136648. doi:10.1016/j.physletb.2021.136648.
- [54] T. H. R. Skyrme, The effective nuclear potential, *Nuclear Phys. B* 9 (1958) 615–634. doi:10.1016/0029-5582(58)90345-6.
- [55] A. S. Umar, M. R. Strayer, P.-G. Reinhard, Resolution of the Fusion Window Anomaly in Heavy-Ion Collisions, *Phys. Rev. Lett.* 56 (1986) 2793–2796. doi:10.1103/PhysRevLett.56.2793.
- [56] A. S. Umar, M. R. Strayer, P.-G. Reinhard, K. T. R. Davies, S.-J. Lee, Spin-orbit force in time-dependent Hartree-Fock calculations of heavy-ion collisions, *Phys. Rev. C* 40 (1989) 706–714. doi:10.1103/PhysRevC.40.706.
- [57] G. Dai, L. Guo, E. Zhao, S. Zhou, Effect of tensor force on dissipation dynamics in time-dependent Hartree-Fock theory, *Sci. China Phys.* 57 (2014) 1618–1622. doi:10.1007/s11433-014-5536-8.
- [58] P. D. Stevenson, E. B. Suckling, S. Fracasso, M. C. Barton, A. S. Umar, Skyrme tensor force in heavy ion collisions, *Phys. Rev. C* 93 (2016) 054617. doi:10.1103/PhysRevC.93.054617.
- [59] L. Guo, C. Simenel, L. Shi, C. Yu, The role of tensor force in heavy-ion fusion dynamics, *Phys. Lett. B* 782 (2018) 401–405. doi:10.1016/j.physletb.2018.05.066.
- [60] L. Guo, K. Godbey, A. S. Umar, Influence of the tensor force on the microscopic heavy-ion interaction potential, *Phys. Rev. C* 98 (2018) 064607. doi:10.1103/PhysRevC.98.064607.
- [61] K. Godbey, L. Guo, A. S. Umar, Influence of the tensor interaction on heavy-ion fusion cross sections, *Phys. Rev. C* 100 (2019) 054612. doi:10.1103/PhysRevC.100.054612.
- [62] X.-X. Sun, L. Guo, A. S. Umar, Microscopic study of the fusion reactions  $^{40,48}\text{Ca} + ^{78}\text{Ni}$  and the effect of the tensor force, *Phys. Rev. C* 105 (2022) 034601. doi:10.1103/PhysRevC.105.034601.
- [63] G. Colò, H. Sagawa, S. Fracasso, P. F. Bortignon, Spin-orbit splitting and the tensor component of the Skyrme interaction, *Phys. Lett. B* 646 (2007) 227–231. doi:10.1016/j.physletb.2007.01.033.
- [64] E. Chabanat, P. Bonche, P. Haensel, J. Meyer, R. Schaeffer, A Skyrme

parametrization from subnuclear to neutron star densities Part II. Nuclei far from stabilities, Nucl. Phys. A 635 (1998) 231–256. doi:10.1016/S0375-9474(98)00180-8.

- [65] D. M. Brink, F. Stancu, Skyrme density functional description of the double magic  $^{78}\text{Ni}$  nucleus, Phys. Rev. C 97 (2018) 064304. doi:10.1103/PhysRevC.97.064304.
- [66] E. B. Suckling, P. D. Stevenson, The effect of the tensor force on the predicted stability of superheavy nuclei, EPL 90 (2010) 12001. doi:10.1209/0295-5075/90/12001.
- [67] A. S. Umar, V. E. Oberacker, Three-dimensional unrestricted time-dependent Hartree-Fock fusion calculations using the full Skyrme interaction, Phys. Rev. C 73 (2006) 054607. doi:10.1103/PhysRevC.73.054607.
- [68] Kazuyuki Sekizawa, Kazuhiro Yabana, Time-dependent Hartree-Fock calculations for multinucleon transfer processes in  $^{40,48}\text{Ca} + ^{124}\text{Sn}$ ,  $^{40}\text{Ca} + ^{208}\text{Pb}$ , and  $^{58}\text{Ni} + ^{208}\text{Pb}$  reactions, Phys. Rev. C 88 (2013) 014614. doi:10.1103/PhysRevC.88.014614.
- [69] J. A. Maruhn, P.-G. Reinhard, P. D. Stevenson, A. S. Umar, The TDHF Code Sky3D, Comput. Phys. Commun. 185 (2014) 2195–2216. doi:10.1016/j.cpc.2014.04.008.
- [70] D. A. Pigg, A. S. Umar, V. E. Oberacker, Eulerian rotations of deformed nuclei for TDDFT calculations, Comput. Phys. Commun. 185 (2014) 1410–1414. doi:10.1016/j.cpc.2014.02.004.